



# Enhancing Radiological Emergency Response Through Agent-Based Model Case 2: Time Required for Staff Assemble

Geon Kim<sup>1</sup> · Jinkyun Park<sup>2</sup> · Gyunyoung Heo<sup>1</sup>

Received: 25 April 2024 / Revised: 10 July 2024 / Accepted: 12 July 2024

© The Author(s), under exclusive licence to Korean Institute of Chemical Engineers, Seoul, Korea 2024

## Abstract

As society becomes more complex, the importance of quick and effective emergency response systems gets more emphasized. This paper introduces a way to reduce the time it takes for emergency staff assembly to be handled during radioactive accidents, which is one of significant factors to manage early stage situations. Using a type of computer modeling called agent-based modeling (ABM) on the NetLogo software, we examine how emergency responses are carried out, focusing on how emergency staff assembly workers are sent out and how they work together in a simulated setting. By integrating traffic and path-finding models, along with real-world GIS (Geographic Information System) data, our methodology allows for more realistic evaluation of response times under various scenarios, including harsh weather conditions (e.g., Heavy snow) and infrastructural disruptions (e.g., Earthquake). The findings reveal significant variability in emergency staff assembly times, underscored by the impact of environmental factors. This research not only contributes to the understanding of emergency response mechanisms but also provides a practical framework for improving the efficacy of disaster management systems, thereby enhancing public safety and resilience against future radiological events.

**Keywords** Emergency response · Agent-based model · Emergency staff assembly time · Real-world tuning

## Introduction

The Fukushima nuclear disaster has underscored the critical importance of rapid and effective emergency response mechanisms [1]. In the aftermath of such incidents, substantial focus has been placed on evacuation strategies, with numerous studies aiming to optimize evacuation processes and accurately predict evacuation times [2–4]. However, while the evacuation of general public is crucial, equally important is the rapid assembly of emergency staff required to stabilize the affected nuclear power plant. The NUREG-CR7002 report includes various factors that affect people's interactions following a nuclear power plant accident. In the USA, this report is used to estimate evacuation times. However, the report relies solely on these factors, making real-time estimation somewhat challenging due to the lack

of visualization and quantification [5]. Recognized within South Korea's Accident Management Program [6], the guidelines specify that emergency staff assembly must be completed swiftly to ensure effective incident management. However, it would be reasonable that the variability and/or uncertainty of such results (emergency staff assembly time) is quantified to control and optimize emergency responses.

Particularly challenging is the scenario of complex disasters, such as the combination of an earthquake with a radiological emergency, which introduces significant variability in emergency staff assembly times. These situations could escalate from a site-specific area alert (blue alert) to a general emergency (red alert), complicating the measurement of specific assembly times.

This study aims to address this gap using an agent-based model to understand the distribution of emergency staffs' assembly times. Agent-based modeling, chosen for its ability to simulate complex interactions among multiple agents and their environment, allows us to observe emergent patterns in emergency staff assembly under varied and uncertain conditions. This methodology is not only applicable to nuclear power plant accidents but can also extend to evacuation plans for chemical accidents, underscoring its utility in

✉ Gyunyoung Heo  
gheo@khu.ac.kr

<sup>1</sup> Department of Nuclear Engineering, College of Engineering, Kyung Hee University, Yongin, Republic of Korea

<sup>2</sup> Risk Assessment Research Team, Korea Atomic Energy Research Institute, Daejeon, Republic of Korea

broader emergency response planning [7]. Various tools support agent-based modeling, and the tool selection was based on considerations of the simulation's purpose and scale, the tool's performance, and scalability. Ultimately, NetLogo was chosen due to its convenience and visualization capabilities.

We have previously developed an evacuation simulation platform, Platform for Radiological SiMulation (PRISM) [8], using NetLogo. While in this context, we simulated large-scale population movements and the possibility of radiation exposure, this study has developed a simulation capable of measuring the emergency staff assembly times in all emergency situations by modifying the previous platform, PRISM, and it was named as PRISM-EC (Emergency Call). By applying existing traffic models (Chapter 2–2. A) and path-finding models (Chapter 2–2. B), and implementation of these methodology to GIS data which fundamental method to develop agent-based model simulation (Chapter 2–2. C), we have developed a more accurate simulation, such that the assembly time can be predicted in various hypothetical situations. We demonstrated the capability of PRISM-EC for several cases and also attempted to verify the suggested methods in Chapter 3.

## Methodology

### Development Environment

In this study, we utilize Agent-Based Modeling (ABM) to analyze the distribution of assembly times for emergency technical support teams during a radiological accident. ABM is a computational approach that models complex phenomena by simulating interactions at the individual agent level [9–12]. This method is particularly suited to scenarios where phenomena are highly interdependent and too complex for traditional equation-based models.

Defining human behavior and decision-making within these scenarios challenges conventional approaches. ABM offers an alternative by allowing us to simulate and iterate through real-world scenarios like fires to identify emergent patterns and solve problems. Unlike traditional methods, ABM does not provide definitive answers but instead explores potential outcomes and situational responses, enhancing our understanding of complex emergency situations.

There are lots of available software options to practically implement ABMs, which brings different pros and cons depending on options. In this study, we utilized a program called Netlogo [13]. Netlogo is fundamentally composed of four types of agents: Turtles, which represent the agents being observed; Patches, which signify environmental changes; Links, which denote interactions; and Observers, who are the observers. These components are aptly

leveraged to model and observe agents, their environments, and their interactions. One function that NetLogo meets the purpose of this study is to offer features for integrating GIS and supports 3D modeling, so that it can provide to reflect various real-world data related to geographic information.

### Traffic and Path-Finding Model

Similar to evacuation simulations, in emergency staff assembly simulations, the exploration of destinations by agents and the traffic model are the most critical elements. Therefore, this chapter provides an explanation of the traffic models and path-finding models on the basis of techniques that have been applied previously, how to implement them into real GIS data.

#### Traffic Model

The traffic model can be considered as a model for how agents (evacuees) move. In this context, a representative model is the Cellular Automata model (hereafter referred to as the CA model) [14]. The CA model overcomes the limitations of macroscopic traffic simulation models, allowing for diverse microscopic traffic simulations. The model is based on the basic unit space occupied by vehicles, known as cells. The state of a cell can take two values: 0 (no vehicle) and 1 (vehicle present). In this study,  $N$  is defined as the sum of all cells representing the number of vehicles on the road. The unit of speed is not the traditional distance per unit time, but rather cells per unit time. The speed of each vehicle can range from 0 to a user-defined value. Figure 1 provides a brief explanation of the CA model.

It is assumed that all roads are subdivided into unit cells. Each vehicle has a forward distance ( $g$ ) available for advancement concerning the leading vehicle and a maximum speed. The maximum speed is defined as  $V_{max}$  in this study. To change lanes, the driver must consider the gap ( $g_p$ ) on the adjacent lane and the distance ( $g_s$ ) to the vehicles in the adjacent lane. Figure 2 shows pseudocode of traffic model about NS-CA (Cellular Automata).

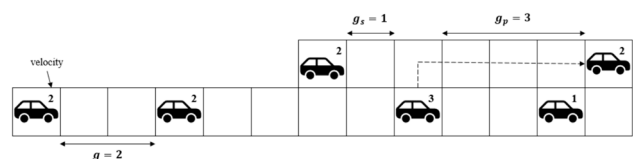


**Fig. 1** A simple model applying the principles of the Cellular Automata (CA) model

**Fig. 2** Pseudocode (NS-CA model)

```

Algorithm NS_CA_Model(road, max_speed, deceleration_probability,
time_steps)
  // Run the simulation for a number of steps
  For each time step in time_steps do
    // Look at each car on the road
    For each car in road do
      // If the car can go faster, increase its speed by 1
      If car's speed < max_speed then
        Increase car's speed by 1

      // Check how far away the next car is
      distance_to_next_car <- Calculate distance to the next
car

      // If the car is too close to the next one, slow down
      If car's speed is more than or equal to
distance_to_next_car then
        Reduce car's speed to be one less than
distance_to_next_car

      // Sometimes, the car randomly slows down a little
      If random chance < deceleration_probability then
        Decrease car's speed by 1

      // Move the car forward based on its current speed
      Update car's position by adding its speed

    // The simulation shows where all cars are after the time steps

Function Calculate distance to the next car(car)
  // Returns the distance from one car to another car ahead

```

### Path-Finding Model

The path-finding model can be considered as a model for determining the direction that agents (evacuees) should take when moving. Search techniques involve methods for finding paths to reach a goal. Search techniques can be classified into blind search and heuristic search methods. Blind search methods sequentially visit possible states without any information, with examples including depth-first search and breadth-first search. When the state space, such as a real-world road network, becomes very large, blind search methods are computationally inefficient and may not provide the optimal path. To address this, heuristic methods introducing state transition costs or search costs can be used.

In this study, we analyzed and applied the A\* algorithm, a representative heuristic algorithm commonly used in traffic navigation. The A\* algorithm searches for the optimal path using an evaluation function, as shown in Eq. 1 [15] [16]

$$f(M) = g(M) + h^*(M). \quad (1)$$

Here,  $g(M)$  represents the distance traveled from the initial node to node  $M$  (the current node), and  $h^*(M)$  signifies the estimated distance from the node to the target node. Heuristic search techniques fundamentally compare the costs incurred when transitioning between states or moving to the next node to determine the next path. The A\* algorithm introduces the estimated future cost, denoted as,  $h^*(M)$  to

reduce unnecessary node visits during this process. Figure 3 illustrates the path-finding flowchart of the A\* algorithm [17]

Also, Fig. 4 shows the pseudocode of A\* algorithm.

### Implementation to GIS

To apply the methodology described above and develop simulations, GIS data are essential. This is an inevitable component for both evacuation and emergency staff assembly. The presence of roads is a fundamental premise that enables people to evacuate or respond to emergency staff assemblies.

The foundational data for modeling were obtained from the GIS data provided by the Ministry of Land, Infrastructure, and Transport [18]. GIS data are comprised

```

Algorithm A_Star(start, goal)
OPEN ← {start}
CLOSED ← {}

while OPEN is not empty do
  current ← node in OPEN with the lowest f_cost
  if current is goal then
    return ReconstructPath(current)

  move current from OPEN to CLOSED

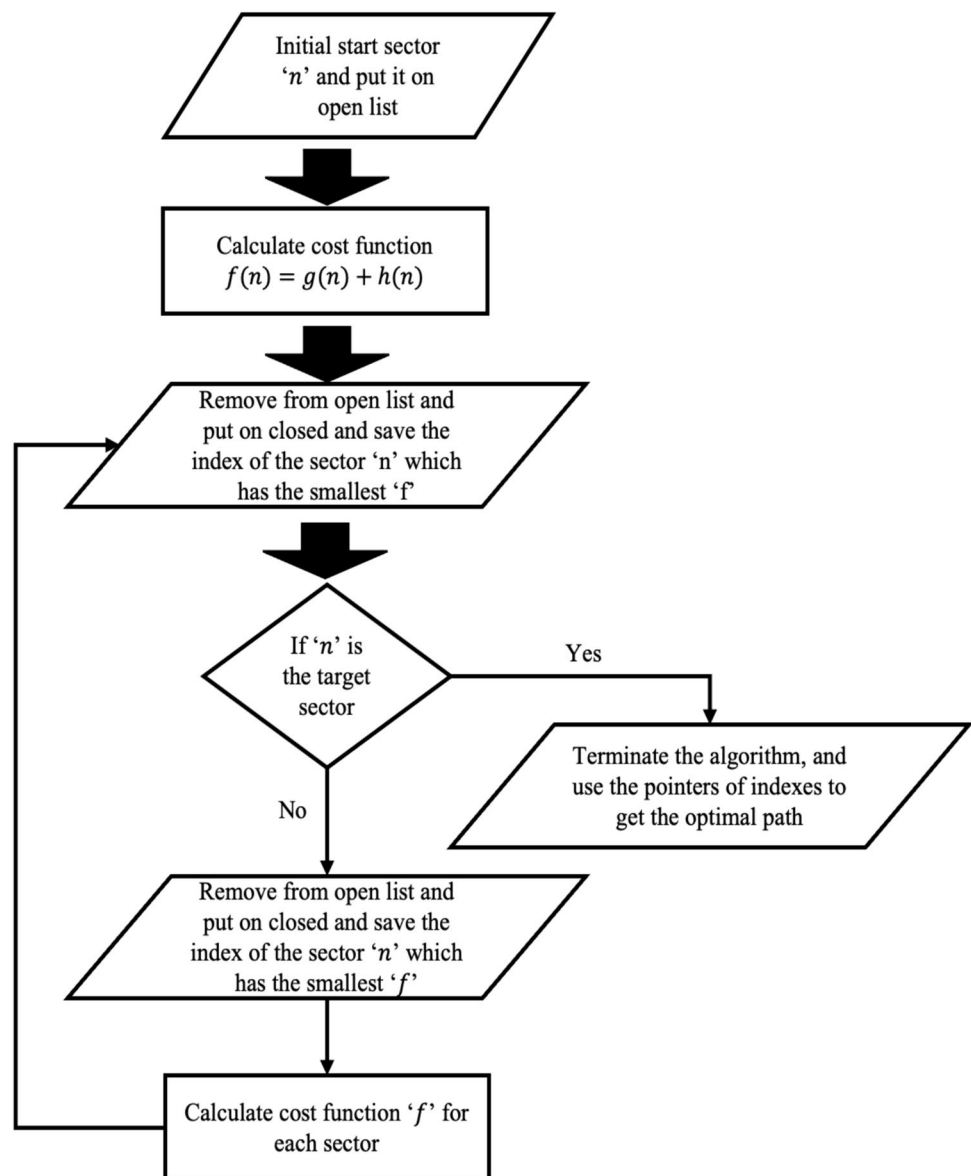
  for each neighbor of current do
    if neighbor not in CLOSED and new path is better
then
      record new path to neighbor
      add neighbor to OPEN if not already in

return failure
  
```

Fig. 4 Pseudocode (A\* algorithm)

of graphic data and attribute data, which are linked to represent geographic information. For vector-type GIS data, discrete geographical features such as roads and

Fig. 3 Flowchart (A\*algorithm) [17]



buildings are expressed in graphic data as points, lines, and polygons, and attribute data consisting of x, y coordinates and other characteristic values are assigned to each graphic element.

In this study, we acquired and modified GIS Data. We aimed to apply the previously described traffic model (Cellular Automata) and path-finding model (A\* algorithm). Specific application examples are as follows. First, to apply the traffic model, the lanes of the roads were newly defined according to the type of road (roads, highways, and alleys). Furthermore, by editing the GIS Data, roads were divided into desired unit cells to enable the reflection of a more accurate traffic model. Next, to apply the path-finding model, a maximum speed was newly defined as an attribute data for each type of road. The A\* algorithm assigns a weight factor to each node, and in this study, each unit cell is defined as a node, with the maximum speed represented as the weight factor ( $g(x)$ ). The heuristic value ( $h(x)$ ) is defined as the straight-line distance between the starting point and the destination. Table 1 presents the attribute data composed of newly defined content combined with existing GIS data.

### Tuning Using Real-World Information (Reference Model)

In this chapter, we aim to explain a technique to the modified model, PRISM-EC. To emphasize the distinctions from the platform PRISM, developed for basic evacuation simulations, it has been named PRISM-EC. In this paper, we named it "Reference model," which is tuned using real-world information. As the name suggests, the goal is to create a model that can serve as a reference when conducting evacuations or making emergency staff assemblies, thereby enhancing accuracy in terms of the duration of time (i.e., emergency staff assembly time). The method to increase accuracy involves verifying the actual traffic volume using commercial GPS and then applying these data to the modified model. The explanation will proceed in the order of describing how commercial GPS data are applied first, followed by how this was implemented in the developed modified model.

**Table 1** Modified GIS Data

Road type	Distance [m]	Number of lanes	Maximum speed
Road	10	2	60
Highway	50	6	100
Alley	3	1	40
⋮	⋮	⋮	⋮

### Traffic Tuning

The reference model can be defined as a condition reflecting the usual road situations. This study considers the emergency staff assembly during a white alert. During a white alert, residents continue their daily activities as usual. Therefore, to develop a traffic model in PRISM-EC, it is necessary to calibrate for traffic volume and speed that mimic normal, everyday conditions. First, using the traffic model (CA model) and path-finding model (A\* algorithm) described earlier, the modified model calculates the time between an arbitrary starting point and destination. Let us assume that this value is denoted as  $t_{sim}$ . Next, the time between the same starting and destination points is derived using commercial GPS (e.g., Kakao maps [19] Google maps [20]). This value is assumed to be  $t_{ref}$ .

Consequently, there will be a difference between values  $t_{sim}$  and  $t_{ref}$ . This discrepancy arises mainly for two reasons: first, because simulations and reality differ, and second, because it is challenging to reflect traffic volume and jam in simulations. To address this, adjustments were made by arbitrarily modifying the number of vehicles on the road and the maximum speed of the road in the simulation. The content explained so far can be represented by Eqs. 2, 3

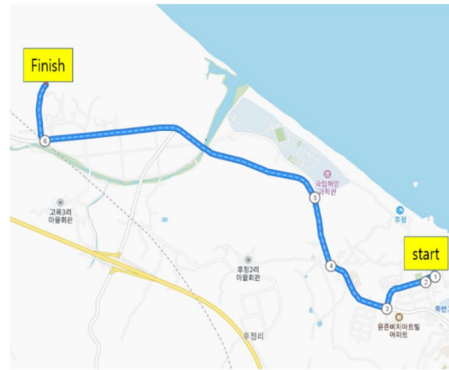
$$N^*, V_{max}^* = \underset{N, V_{max}}{argmin} |t_{sim} - t_{ref}| \tag{2}$$

$$t_{sim} = \text{Traffic model}(A^*, N, V_{max}). \tag{3}$$

In the equation,  $N$  represents the number of vehicles on a typical road within the Netlogo program, and  $V_{max}$  signifies the maximum speed of vehicles within the program. Therefore, the equation can be interpreted as finding the values of  $N$  and  $V_{max}$  that minimize the difference between  $t_{sim}$  and  $t_{ref}$ .

However, we encountered difficulties in finding the appropriate value for  $t_{ref}$ . To obtain this value, we utilized web crawling techniques [21]. In this paper, we developed a Python program. When executed, the program activates commercial GPS at designated times and retrieves the vehicle travel time between arbitrarily chosen starting and destination points as the output. This output can be directly obtained in a csv file. In this study, we extract time values daily at 08:00, 14:00, 18:00, and 03:00, which are important points in the daily schedule. As explained later in Chapter 2–3. B, we will combine them with yearly weather information. This combination involves the calibration of road data, which is crucial for estimating assembly time. Using these data, we calibrated the models between  $t_{ref}$  and  $t_{sim}$  by minimizing the difference between the two values, as explained in Eq. 2.

**Fig. 5** Start-finish point (right) and results (left)



YY-MM-DD	Time	Min
2024-04-03	18:00:02	10
2024-04-04	3:00:02	9
2024-04-04	8:00:02	9
2024-04-04	12:00:02	9
2024-04-04	18:00:02	9
2024-04-05	3:00:02	9
2024-04-06	8:00:02	9
2024-04-07	12:00:02	10

Figure 5 displays the data for origin–destination points obtained through web crawling, along with the compiled times. Figure 6 illustrates algorithm which was developed by python programming. The initial step involves interfacing with a commercial GPS system to set the destination and determine the arrival position. Once the connection is established, the program concurrently extracts two pivotal datasets: optimal travel time data, reflecting real-time traffic conditions, and the current time as registered within the Python code environment. A critical user-defined parameter, the target time, is then set, which represents the temporal boundary for the program's operation. With the parameters in place, the program commences outputting optimal time data at consistent hourly intervals.

**Weather Tuning**

As other factors to improve accuracy of PRISM-EC, we tuned algorithms using real-world weather conditions, observing how results can vary even on the same day, depending on the weather. For example, on a snowy day in January, the travel time obtained from commercial GPS is expected to increase compared to other days. This is a well-known fact. By applying this understanding, we can derive more accurate simulation results under a variety of conditions.

Over approximately 8 months, the travel times between arbitrary starting points and destinations were obtained using the values outputted to a spread sheet. Furthermore, by entering the most representative place names near the arbitrary starting points and destinations into the Korea Meteorological Administration [22], the hourly weather for the day can be acquired. Then, the corresponding weather is recorded in the spread sheet, matched to the times we have designated. Figure 7 shows a Korean weather site from which one can obtain hourly weather information provided by the Korea Meteorological Administration.

Thus, this study compares travel times at different times of the same day to approximate the actual values of  $N$  and  $V_{max}$ . Table 2 shows an example of a complete reference model using the data we have.

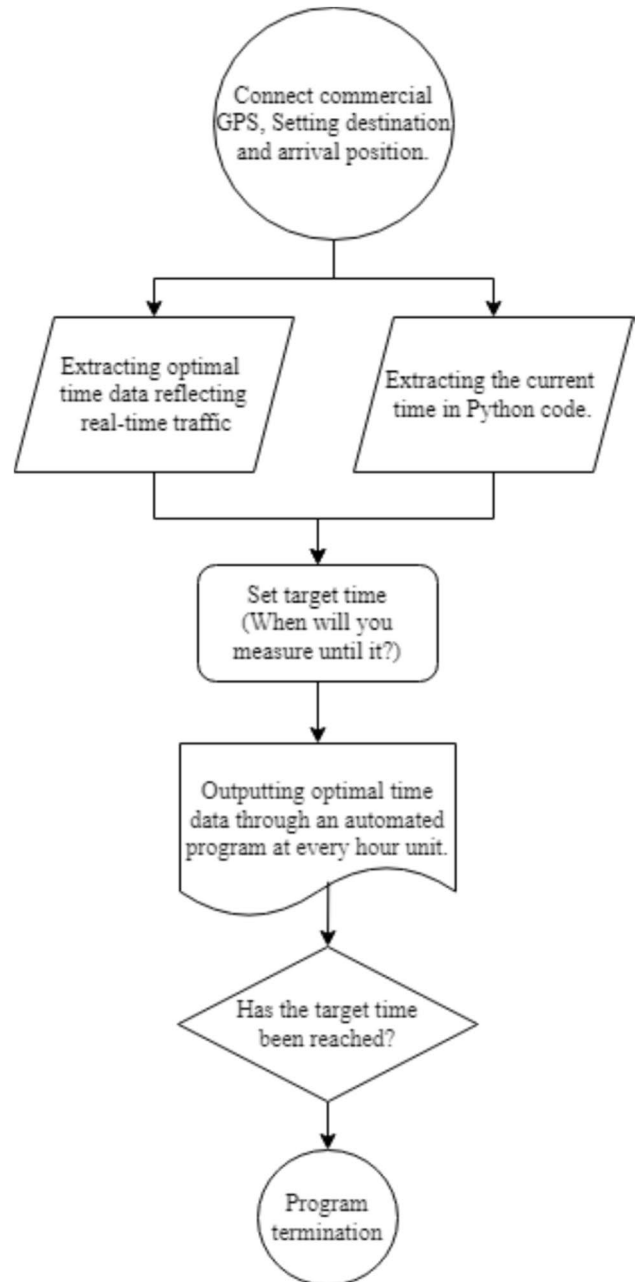
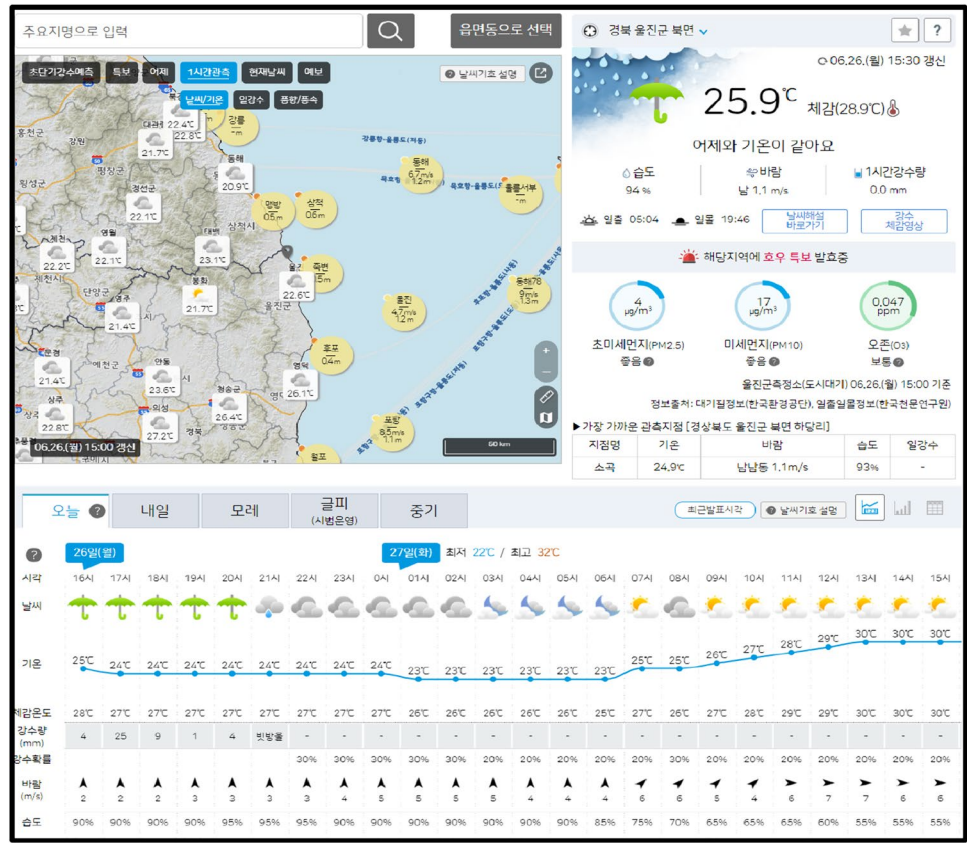


**Fig. 6** Web crawling program algorithm (Python)

Fig. 7 Korea Meteorological Administration website



By utilizing these data to adjust  $N$  and  $V_{max}$  according to the seasons and times of day, and using Eq. 2 defined in the previous chapter, we could minimize the difference between the  $t_{ref}$  and  $t_{sim}$  values (Eq. 3). This model implements two tuning strategies that incorporate real-world information on weather and traffic. This method may increase accuracy to levels more closely resembling actual situations.

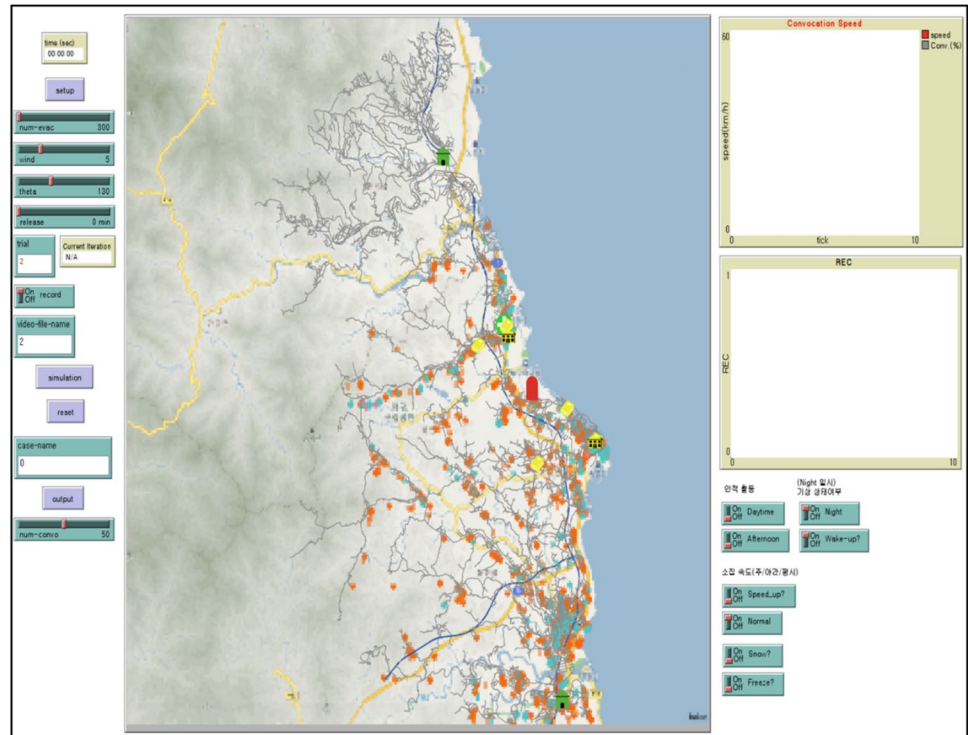
### Results and Discussion

Finally, PRISM-EC with an implemented reference model was developed. The completed PRISM-EC can be represented as shown in Fig. 8. A simulation video concerning the reference case has been published at “<https://youtu.be/VlszSEQW9Sg>”.

Table 2 Example of complete reference model

Seasons ( $i$ )/time ( $j$ ) and weather ( $k$ )	Spring ( $i=1$ )	Summer ( $i=2$ )	Autumn ( $i=3$ )	Winter ( $i=4$ )
<Type>				
Clear ( $k=1$ )	Morning (08:00) ( $j=1$ )	$N_{111}^*, V_{111max}^*$	...	$N_{411}^*, V_{411max}^*$
Snow ( $k=2$ )		$N_{112}^*, V_{112max}^*$	...	$N_{412}^*, V_{412max}^*$
Rain ( $k=3$ )	Daytime (14:00) ( $j=2$ )	$N_{113}^*, V_{113max}^*$	...	$N_{413}^*, V_{413max}^*$
	Evening (18:00) ( $j=3$ )	...	$N_{ijk}^*, V_{ijkmax}^*$	...
	Night (20:00) ( $j=4$ )	$N_{141}^*, V_{141max}^*$	...	$N_{441}^*, V_{441max}^*$
		$N_{142}^*, V_{142max}^*$		$N_{442}^*, V_{442max}^*$
		$N_{143}^*, V_{143max}^*$		$N_{443}^*, V_{443max}^*$

**Fig. 8** Example of PRISM-EC (Simulation start)



## Simulation Environment

The interface has been enhanced with the following features: a real-time measuring timer, the number of general population ( $N$ ), the number of emergency staff assembly agents, and the number of repetitions as input values. Additionally, the right graph and the On/Off function are output values, representing the average speed of the emergency staff assembly agent and the extent to which the influence factor is reflected. This study aimed to apply all the variables considered in the previous chapter. Two scenarios are presented as examples to investigate the distribution of emergency staff assembly time.

First, the distribution of emergency staff assembly time under the most basic reference case (spring, clear, daytime) currently applied in PRISM-EC is simulated. Second, the distribution of emergency staff assembly time during natural disaster involving both an earthquake and heavy snow is examined. The number of simulations was set to 50 for each scenario.

## Reference Case

The first result is as follows: The distribution of emergency staff assembly time under the reference case (Clear, Daytime, and Spring in the Reference model) can be represented in Fig. 9. In this paper, the reference case is defined in relation to specific weather conditions (Clear, Daytime, and Spring). We collected raw data using a Python script

to perform web crawling, capturing the required time every day during about 1 year.

The number of simulation iterations is 50. The simulation data were fitted to a log-normal distribution to refine the data. The data were fitted to a log-normal distribution with parameters  $\mu = 2.257$ ,  $\sigma = 0.044$ , which provided the average and standard deviation of the distribution. The probability density function of the fitted log-normal distribution is given by Eq. 4

$$f(x;2.257,0.044) = \frac{1}{0.0044\sqrt{2\pi x}} e^{-\frac{(\ln x - 2.257)^2}{0.003872}} \text{ for } x > 0. \quad (4)$$

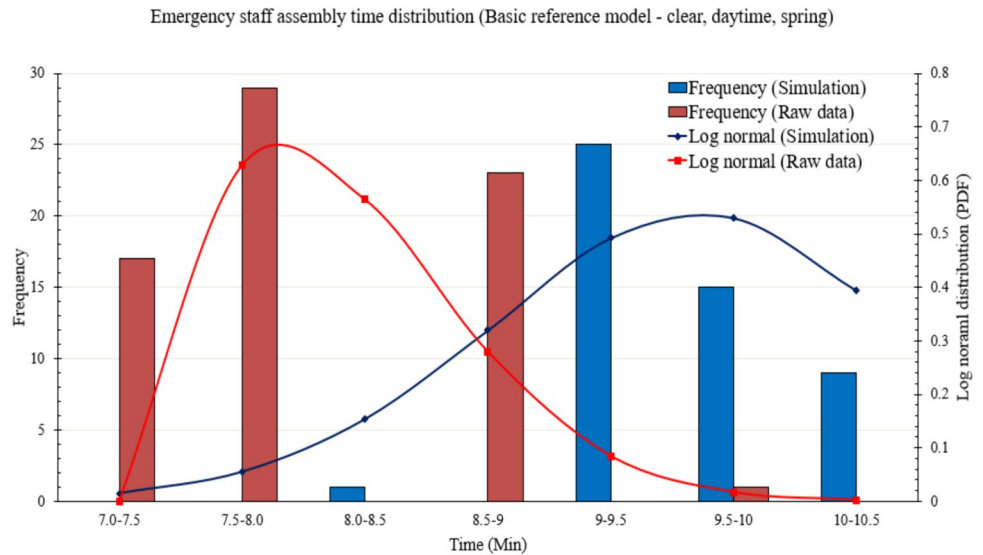
The average emergency staff assembly time is 9.281 min, with a standard deviation of 0.359 min. The standard deviation arises due to slight variations in path-finding with each trial. To verify this result, we used raw data obtained from web crawling. The data were fitted to a log-normal distribution with parameters  $\mu = 2.071$ ,  $\sigma = 0.100$ , which provided the average and standard deviation of the distribution. The probability density function of the fitted log-normal distribution is given by Eq. 5

$$f(x;2.071,0.100) = \frac{1}{0.1\sqrt{2\pi x}} e^{-\frac{(\ln x - 2.071)^2}{0.02}} \text{ for } x > 0. \quad (5)$$

The average time was 8.114 min, with a standard deviation of 0.790 min. As illustrated in Fig. 9, the simulation data are left-skewed. This skewness may result



**Fig. 9** Emergency staff assembly time distribution (basic reference model)



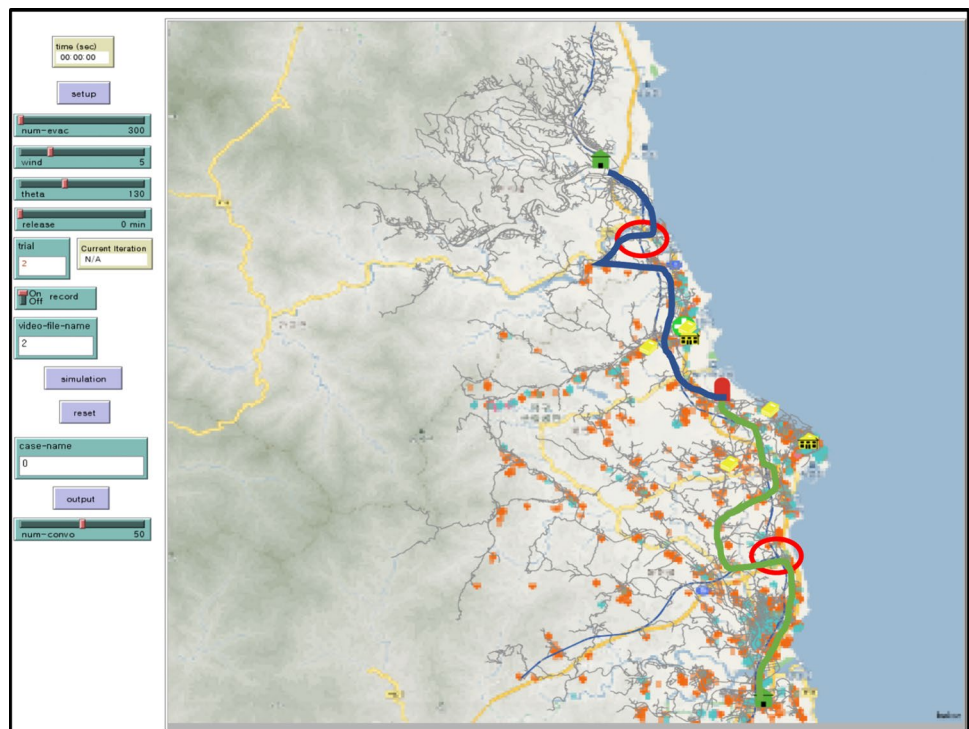
from insufficient simulation data or minor errors during the tuning of PRISM-EC. Despite this, the shape of the log-normal distribution remains similar, which supports the verification of PRISM-EC. Consequently, although there are differences between the current reference case and the raw data, they exhibit a similar shape when plotted as a log-normal distribution. This similarity indicates that the reference case values are comparable to the raw data.

**Case Study 1: Earthquake**

The second result is as follows: The distribution of emergency staff assembly time during a complex disaster, namely an earthquake and a radiation emergency, is represented in Fig. 10. Initially, to simulate the impact of the earthquake, two roads were removed before starting the simulation.

The reasons for selecting two roads are as follows. First, these roads are most frequently used by emergency staff assembly agents when searching for routes using a

**Fig. 10** Remove 2 roads (Blue, Green line: detour route)



path-finding model. Removing these would mean losing the shortest possible routes, clearly leading to detours. Second, since detours consist of general roads and alleyways, it is anticipated that vehicles will experience deceleration or stopping due to the traffic model. For these reasons, the decision was made to remove two roads.

Moreover, when more than five roads were removed, there were instances where the path-finding model did not apply correctly, resulting in the inability to find a path. The average emergency staff assembly time required was 27.74 min, with a standard deviation of 1.902 min through 50 simulation iterations. This increase can be attributed to the rerouting of many vehicles due to the roads that were cut during the simulation.

The simulation data (Fig. 11) was fitted to a log-normal distribution to refine the data. The data were fitted to a log-normal distribution with parameters  $\mu = 3.445, \sigma = 0.059$ , which provided the average and standard deviation of the distribution. The probability density function of the fitted log-normal distribution is given by Eq. 6

$$f(x;3.445, 0.059) = \frac{1}{0.059x} e^{-\frac{(\ln x - 3.445)^2}{0.00696}} \text{ for } x > 0. \quad (6)$$

To verify this result, we additionally collected data using the detour function in commercial GPS, where cars used alternative routes to reach the nuclear power plant if roads were closed. Figures 12 and 13 show the assembly times obtained from a commercial GPS. On the left, the times are shown for the normal case where the roads are not closed, while on the right, the times for the case where

the roads are closed and detours are taken are displayed. For Fig. 12, it took approximately 27 min in case of the road blocked. While for Fig. 13, it took around 15 min. Since our developed PRISM-EC predicts the time when all emergency personnel have arrived, the assembly time due to detours can be defined as 27 min, which serves as the raw data. Unlike the raw data used in the reference case, the data collected here are less extensive. To compare the actual data with the simulation results, we calculated the relative error, which was found to be 2.741%. Assuming that this difference is negligible, this value suggests that the simulation data from PRISM-EC are similar to the actual raw data. Furthermore, it was observed that the values increased by approximately 2.5 times when compared to the simulation results from the reference case (Chapter 3–2). This is similar to the time increment shown in Figs. 12 and 13

$$\text{Relative error} = \frac{|(\text{Simulation data}) - (\text{Raw data})|}{(\text{Raw data})}. \quad (7)$$

In Case Study 1, assuming the occurrence of an earthquake, we simulated this scenario by arbitrarily blocking two roads within PRISM-EC. This represents a limitation of the current implementation, as it does not fully capture the complexity of a real earthquake event. In reality, an actual earthquake would likely involve numerous additional factors and challenges. Therefore, further modeling and enhancements would be required to more accurately reflect the multifaceted nature of earthquake impacts and emergency response scenarios.

**Fig. 11** Emergency staff assembly time distribution (earthquake + radiological accident)

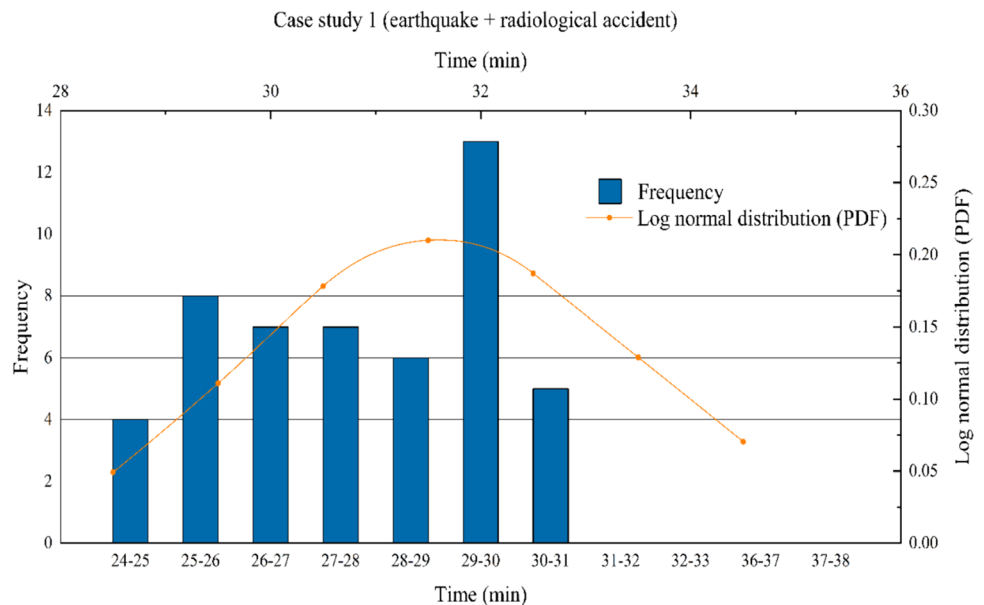


**Fig. 12** Detour route 1 (13 min → 27 min)

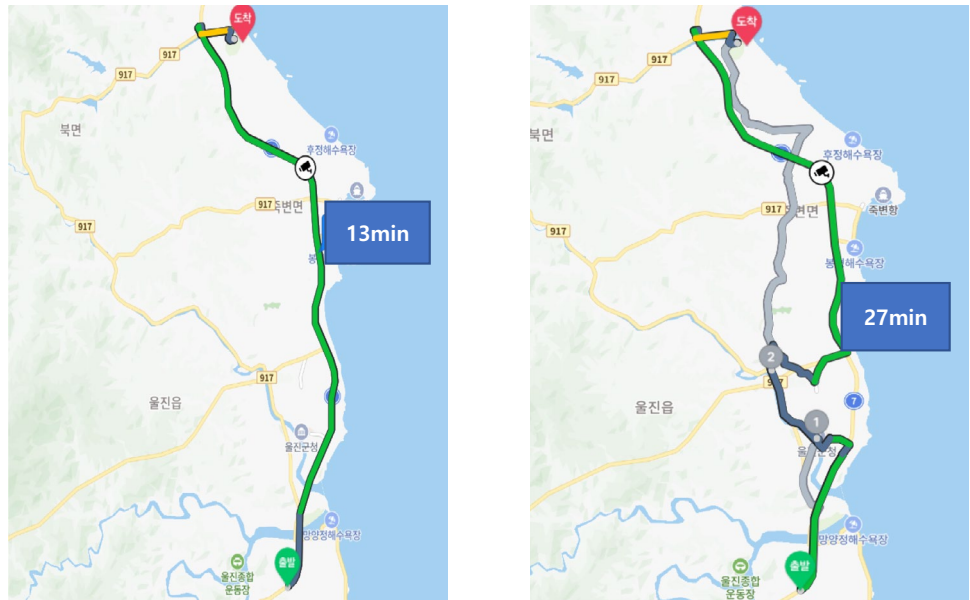
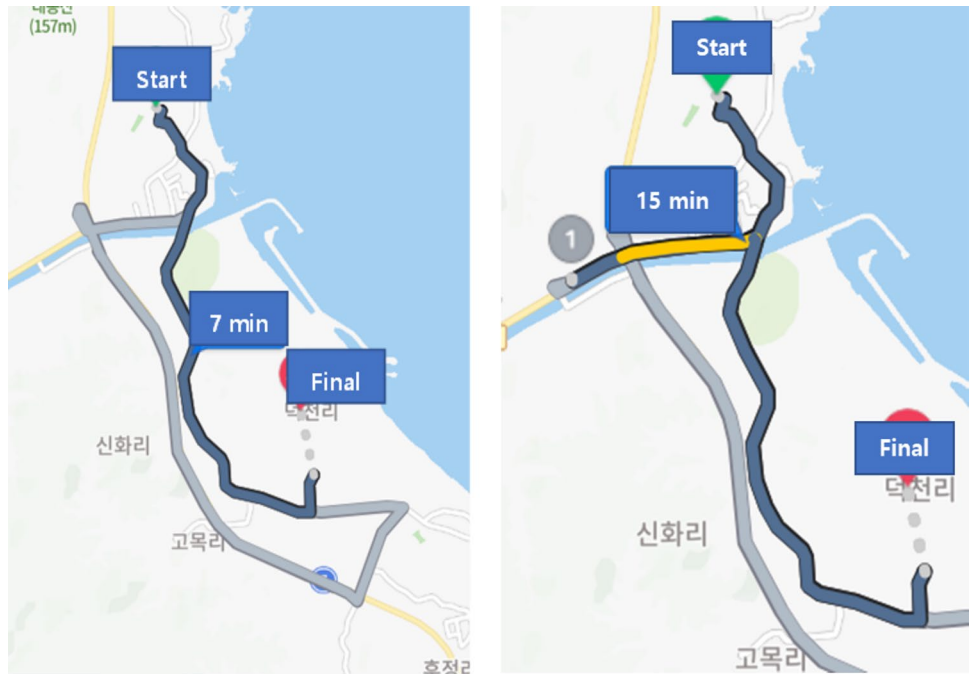


**Fig. 13** Detour route 2 (7 min → 15 min)

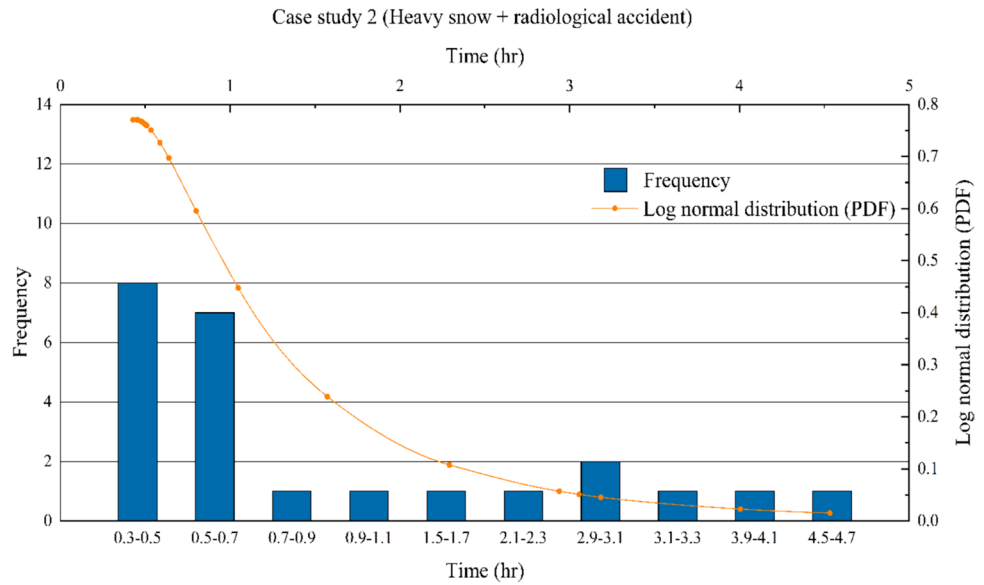


**Case Study 2: Heavy Snow**

The emergency staff assembly response time data in the histogram (Fig. 14), which deals with a scenario of heavy snowfall combined with a radiological accident, provides critical insights into the response efficiency under these extreme conditions. During this event, heavy snow refers to a situation where snow causes significant difficulties in vehicle movement, resulting in severe speed reductions and traffic congestion. A deeper analysis of the dataset reveals that the average emergency staff assembly time was approximately

1.289 h, with a significant standard deviation of 1.260 h. This substantial spread in the data underscores the unpredictability and severity of the conditions affecting response times. The contributing factors to the increased emergency staff assembly times and standard deviation can be ascribed to several interlinked issues. Predominantly, the heavy snow led to impassable roads in many areas, creating prolonged situations where vehicular movement was not just impeded but completely halted. This standstill is depicted in the frequency of emergency staff assemblies except in the 0.3–0.7 h range.

**Fig. 14** Emergency staff assembly time distribution (heavy snow + radiological accident)



In this case, the number of simulation’s iteration was 25. The simulation data were fitted to a log-normal distribution to refine the data. The data were fitted to a log-normal distribution with parameters  $\mu = -0.129, \sigma = 0.815$ , which provided the average and standard deviation of the distribution. The probability density function of the fitted log-normal distribution is given by Eq. 8

$$f(x; -0.129, 0.815) = \frac{1}{0.815\sqrt{2\pi x}} e^{-\frac{(\ln x + 0.129)^2}{1.328225}} \text{ for } x > 0. \quad (8)$$

In case of heavy snow, observational data corroborated a drastic reduction in average vehicle speed, which plummeted to 20–30% of the speeds noted in standard conditions reflected in the reference model. This deceleration was not a linear decrease across all areas but varied significantly, as the traffic model indicates a bottleneck effect. In several instances, the traffic flow was disrupted, leading to a cascade of delays that amplified the time required for emergency responders to reach their maximum permissible speeds. The slowdown in vehicle movement was further exacerbated by the accumulated snow on the roadways. The histogram also reveals several outliers, where emergency staff assembly times extended beyond 3 h. Overall, the analysis of these data not only illustrates the direct effects of compounded emergency scenarios on response times but also highlights the complex interplay between environmental conditions and infrastructure limitations.

In the reference case (Chapter 3–2) and Case Study 1 (Chapter 3–3), verification was conducted by collecting raw data through commercial GPS and comparing these data. However, Case Study 2 will employ a different verification approach for two primary reasons. First, the raw data collected, as used in Chapter 3–2, were

insufficient to accurately represent the conditions of a heavy snowfall scenario. Second, experiencing actual heavy snowfall events is inherently challenging, making it difficult to gather relevant data. Therefore, we aim to proceed with verification using a new method to better address these limitations and accurately model the impact of heavy snowfall.

To verify this result, we compared the assembly time for case study 2 with NUREG/CR-7002 [5]. This report includes a table that describes how road conditions change according to weather conditions. Table 3 shows roadway capacity and speed under these conditions.

In this table, the weather condition corresponds to heavy snow. We assumed an increasing rate by multiplying roadway capacity by speed, because the reference model does not have independent measurements for these factors. That is why, we define a new value called the increasing rate. Equation 9 defines and calculates the increasing rate based on Table 3

$$\text{Increasing rate} = \frac{t_{\text{heavy snow}}}{t_{\text{reference}}} = \frac{0.75 * 0.85}{1.0 * 1.0} = 0.63. \quad (9)$$

Also, the increasing rate can be directly calculated using the reference model, since PRISM-EC is able to provide

**Table 3** Road state change due to weather condition

Weather condition	Roadway capacity	Speed
Normal	100%	100%
Rain/light snow	90%	90%
Heavy snow	75%	85%
Fog	90%	85%

the assembly time through simulations. Equation 10 shows the increasing rate based on the simulation results

$$\frac{t_{\text{heavy snow}}}{t_{\text{reference}}} = \frac{28 \text{ min}}{40 \text{ min}} = 0.70. \quad (10)$$

The simulation results demonstrate an increasing rate of 0.7. Furthermore, the relative error between the reported data and the simulation results is approximately within 10%. This value indicates that our simulation results are closely aligned with the reported values. This finding signifies an acceptable range, validating the effectiveness of the simulation process.

## Conclusions

In this study, we aimed to obtain the distribution of emergency staff assembly times for agents during a white emergency, a type of radiation emergency. We investigated the types of emergency organizations involved in a radiation emergency and the factors that could affect their emergency staff assembly times. Additionally, we sought to randomly generate these factors.

Utilizing an agent-based model, we modified the PRISM, to develop an emergency staff assembly simulation (PRISM-EC). To modify the program, we laid the groundwork through a basic preparation process while applying traffic and path-finding models. We also developed a reference model. Using commercial GPS data and Korea Meteorological Administration data, we aimed to significantly improve the objectivity and reliability, which are considered the biggest weaknesses of the current agent-based model. We ran two simple example models using the developed simulation to derive distributions. The results indicated that it was possible to assemble emergency staff within a 3 h timeframe, although no dramatic results were obtained.

Looking ahead, we wish to introduce future topics of interest. By incorporating these results into the reference case, we believe that the program can be effectively used to verify the distribution of emergency staff assembly times in extreme situations where actual drills are difficult. Additionally, we plan to include more diverse factors affecting the emergency staff assembly times of agents to create a more realistic model. Moreover, we aim to further develop this simulation to explore ways to enhance safety in response to multi-unit nuclear power plant accidents. Finally, completing the currently incomplete reference case is the ultimate goal of this research.

Currently, the verification process for our software (PRISM-EC) has only been conducted on a single aspect. However, we aim to demonstrate that it is capable of

continuous updates by incorporating real data. In future work, we plan to compare the figures presented in NUREG-CR7002 with actual data to develop an extensible software capable of producing reliable results under all conditions.

**Acknowledgements** This work was supported by the National Research Foundation of Korea (NRF) grant funded by the Korean government (MSIP: Ministry of Science, ICT and Future Planning) (No. NRF-2021M2D2A1A02044210).

**Funding** This work was supported by the Human Resources Development of the Korea Institute of Energy Technology Evaluation and Planning (KETEP) grant funded by the Ministry of Trade, Industry and Energy of Korea (No. RS-2023–00244330).

## References

1. Nuclear Safety And Security Commission, "Fukushima nuclear accident follow-up and future action plan." Nuclear Safety And Security Commission, N/A, 2014.
2. B. Kim, B. Son, H. Jeon, Evaluation of evacuation strategies according to the travel demand: The case of nuclear research reactor HANARO's EPZ. *Sustainability* **12**(15), 6128 (2020)
3. J. Kim, F. Rukundo, A. Musauddin, B. Tseren, G.M. Uddin, T. Kiplabat, Emergency evacuation simulation for a radiation disaster: A case study of a residential school near nuclear power plants in Korea. *Radiat. Prot. Dosim.* **189**, 323–336 (2020)
4. H. Miao, G. Zhang, P.S.C. Yu, J. Zheng, Dynamic dose-based emergency evacuation model for enhancing nuclear power plant emergency response strategies. *Energies* **16**(17), 6338 (2023)
5. Office of nuclear security and incident response, "Criteria for development of evacuation time estimate studies (NUREG/CR-7002)," United States nuclear regulatory commission, Rockville, 2021.
6. B.-W. Sung, "KHNP accident management program: Organization and Response system," In: *Nuclear Safety & Security Information Conference 2023*, Daejeon, 2023.
7. K.O. Lee, J.Y. Park, C.J. Lee, Evaluation of a mitigation system for leakage accidents using mathematical modeling. *Korean J. Chem. Eng.* **35**, 348–354 (2018)
8. G. Heo and G. Kim, "Agent-based radiological emergency evacuation simulation modeling considering mitigation infrastructures," *Reliability Engineering & System Safety*, pp. 233, 109098, 2023.
9. G. Heo, Y. Hwang, Development of a radiological emergency evacuation model using agent-based modeling. *Nuclear Eng. Technol.* **53**(7), 2195–2206 (2023)
10. J. Pleyer, C. Fleck, Agent-based models in cellular systems. *Front. Phys.* **10**, 968409 (2023)
11. P. Su, M. Chen, Y. Wang, Agent-based model: A method worthy of promotion in library and information science. *J. Inform. Sci.* **49**(6), 1517–1527 (2023)
12. B. Ashrafi, G. Kim, M. B. J. Naseri, S. Dhar, S. Baek, G. Heo, An agent-based modelling framework for performance assessment of search and rescue operations in the Barents Sea. *Saf. Extreme Environ.* **6**(1), 1–18 (2024)
13. U. Wilensky, "NetLogo. Evanston, IL: Center for connected learning and computer-based modeling, Northwestern University," 16 Aug 2022. [Online]. Available: <http://ccl.northwestern.edu/netlogo/>.
14. R. Barlovic, J. Esser, K. Froese, W. Knospe, L. Neubert, M. Schreckenber, J. Wahle, "Online traffic simulation with cellular

- automata, in *Traffic and mobility: Simulation economics environment*. (Springer, Berlin Heidelberg, 1999), pp.117–134
15. R. Dechter, J. Pearl, 1985 Generalized best-first search strategies and the optimality of A\*. *J. ACM (JACM)* **32**(3), 505–536 (1985)
  16. G. Kim, G. Kim, M. Hwang and G. Heo, "Platform for radiological emergency agent-based integrated simulation model," In: *2022 6th International Conference on System Reliability and Safety (ICSRS)*, Venice, 2022.
  17. I. Zidane and K. Ibrahim, "Wavefront and A-Star Algorithms for Mobile Robot Path Planning," In: *Proceedings Of The International Conference On Advanced Intelligent Systems And Informatics 2017*, 2018.
  18. Ministry of land, infrastructure and transport, "DATA.GO.KR," 26 Sept 2023. [Online]. Available: <https://www.data.go.kr/data/15123970/openapi.do?recommendDataYn=Y>.
  19. Kakao co., "Kakao maps," [Online]. Available: <https://map.kakao.com/>. Accessed 1 Aug 2023.
  20. Google, [Online]. Available: <https://www.google.com/maps>. Accessed 1 Aug 2023.
  21. C. Olston, M. Najork, Web crawling. *Found. Trends® Inform. Retr.* **4**(3), 175–246 (2010)
  22. Korea Meteorological Administration, "Korea meteorological administration weather nuri," [Online]. Available: <https://www.weather.go.kr/w/index.do#dong/4793031000>. Accessed 1 Aug 2023.

**Publisher's Note** Springer Nature remains neutral with regard to jurisdictional claims in published maps and institutional affiliations.

Springer Nature or its licensor (e.g. a society or other partner) holds exclusive rights to this article under a publishing agreement with the author(s) or other rightsholder(s); author self-archiving of the accepted manuscript version of this article is solely governed by the terms of such publishing agreement and applicable law.